Specific heat of geometrically frustrated and multiferroic $R\mathrm{Mn}_{1-x}\mathrm{Ga}_x\mathrm{O}_3$ (R=Ho, Y)

H. D. Zhou, J. A. Janik, B. W. Vogt, Y. J. Jo, L. Balicas, M. J. Case, and C. R. Wiebe
Department of Physics, Florida State University, Tallahassee, Florida 32306-3016, USA
and National High Magnetic Field Laboratory, Florida State University, Tallahassee, Florida 32306, USA

J. C. Denyszyn and J. B. Goodenough
Texas Materials Institute, ETC 9.102, The University of Texas at Austin, 1 University Station, C2201, Austin, Texas 78712, USA

J. G. Cheng
Center for Condensed Matter Science and Technology (CCMST), Department of Applied Physics, Harbin Institute of Technology, Harbin 150001, People's Republic of China

(Received 24 April 2006; revised manuscript received 12 July 2006; published 25 September 2006)

Specific heat measurements on single crystals of $R\mathrm{Mn}_{1-x}\mathrm{Ga}_x\mathrm{O}_3$ (R=Ho, Y) have revealed that Ga doping raises the Mn-spin reorientation temperature T_{SR} while lowering the antiferromagnetic ordering temperature, T_N, of the Mn spins and the Ho magnetic ordering temperature T_2. The variations of the calculated magnetic entropy with Ga doping show the existence of spin fluctuations above T_N in the geometrically frustrated Mn-spin system and a coupling between the Mn^{3+}-ion and Ho^{3+}-ion spins both at T_{SR} and T_2. The data also support Schottky anomalies in the specific heat of $\mathrm{HoMn}_{1-x}\mathrm{Ga}_x\mathrm{O}_3$, which is dominated by crystalline electric fields but also affected by Mn^{3+}-ion spin orderings. The large electronic contribution to specific heat of HoMnO_3, γ, is suggested to be due to Ho^{3+} spin disorder.

DOI: 10.1103/PhysRevB.74.094426 PACS number(s): 75.47.Lx, 65.40.Ba, 75.40.−s

INTRODUCTION

The $R\mathrm{MnO}_3$ compounds with smaller rare-earth ions (R from Ho-Lu and Y) have attracted considerable recent attention because of the coexistence of ferrielectricity and antiferromagnetic order with a coupling between them. HoMnO_3, for example, has the following properties: (i) a ferrielectric displacement of the Ho^{3+} ions along the c axis below a Curie temperature T_C=875 K due to a cooperative rotation of the bipyramidal axis from the c axis;[1] (ii) the dominant spin-spin interactions between Mn^{3+} ions within the close-packed basal planes are geometrically frustrated (GF), which lowers the antiferromagnetic ordering temperature T_N of the Mn^{3+} ions to T_N=70 K$\ll T_C$;[2] (iii) a reorientation of the Mn^{3+}-ion spins from perpendicular to the a axis to along the a axis occurs at $T_{SR}\approx$40 K,[3] where a sharp peak in the dielectric constant and partially ordered Ho^{3+}-ion spins have been observed;[4–6] and (iv) another 90° spin reorientation of the Mn^{3+}-ion spins is accompanied by a magnetic ordering of the Ho^{3+}-ion spins orientated along the c axis at $T_2\approx$5 K.[7] Recent work on these $R\mathrm{MnO}_3$ compounds has been focused on magnetic phases at low temperatures[3–10] and the coupling between the ferrielectric and magnetic orderings.[11–14] The nature of the interactions between Mn spins and Ho spins around T_{SR} and T_2, or the possible coupling between the ferrielectric polarization and the Ho^{3+}-ion spin at T_{SR}, are still topics of debate.

This paper reports specific heat (C_p) measurements made on single crystals of $R\mathrm{Mn}_{1-x}\mathrm{Ga}_x\mathrm{O}_3$ (R=Ho, Y) to investigate how the several transition temperatures vary with respect to one another and also how the entropy due to magnetic ordering changes with increasing x. These measurements provide information on the coupling between ferroelectric and magnetic orderings as well as between the Ho^{3+} and Mn^{3+} magnetic ordering. Schottky anomalies are observed for $\mathrm{HoMn}_{1-x}\mathrm{Ga}_x\mathrm{O}_3$, which are common for rare-earth elements; no data has been reported for HoMnO_3. C_p measurements on $\mathrm{YMn}_{1-x}\mathrm{Ga}_x\mathrm{O}_3$ show the existence of spin fluctuations above T_N for a geometrically frustrated (GF) spin system.

EXPERIMENT

Single crystals of $R\mathrm{Mn}_{1-x}\mathrm{Ga}_x\mathrm{O}_3$ (R=Ho, Y and x=0, 0.03, 0.1, 0.2, and 0.3) were grown by the traveling-solvent floating-zone (TSFZ) technique. The feed and seed rods for the crystal growth were prepared by solid-state reaction. Stoichiometric mixtures of $\mathrm{Ho}_2\mathrm{O}_3/\mathrm{Y}_2\mathrm{O}_3$, $\mathrm{Mn}_2\mathrm{O}_3$, and $\mathrm{Ga}_2\mathrm{O}_3$ were ground together and calcined in air at 950 °C for 24 h. The sample was reground and sintered at 1100 °C for another 24 h in air and cooled to room temperature. It was then reground again into a powder and pressed into a 6-mm-diameter×60-mm rod under 400 atm hydrostatic pressure. The rods were finally sintered at 1200 °C for 20 h in air. The crystal growth was carried out in air in an IR-heated image furnace (NEC) equipped with two halogen lamps and double ellipsoidal mirrors. The feed and seed rods were rotated in opposite directions at 25 rpm during crystal growth at a rate of 4 mm/h.

Small pieces of the single crystals were ground into a fine powder for x-ray diffraction (XRD). The room-temperature measurements were recorded with an X-pert Philips diffractometer equipped with Cu K_α radiation. Data were collected in steps of 0.020° over the range $15° \leqslant 2\theta \leqslant 90°$ with a count time of 5 s per step. Peak profiles for the XRD data were refined with the program FULLPROF. All samples were single-phase with the hexagonal $P6_3cm$ structure via XRD.

Samples cut from the single crystals for specific heat measurements had a typical size of $1.5\times1.5\times0.5$ mm^3. The spe-

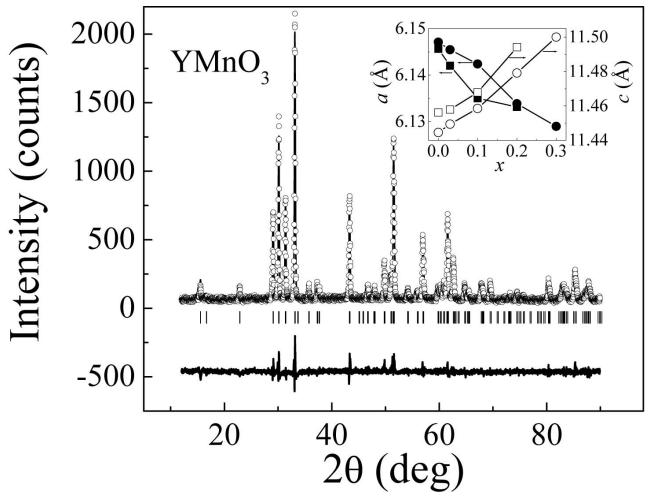

FIG. 1. Room temperature XRD pattern for $YMnO_3$ (open circles plus marks). The solid curve is the best fit from the Rietveld refinement using FULLPROF. The vertical marks indicate the position of Bragg peaks, and the bottom curve shows the difference between the observed and calculated intensities. Inset: Variation of lattice parameters a and c with x for $HoMn_{1-x}Ga_xO_3$ (■: a, □: c) and $YMn_{1-x}Ga_xO_3$ (●: a, ○: c).

cific heat measurements were performed on a PPMS (Physical Property Measurement System, Quantum Design) at temperatures from 2 to 300 K.

RESULTS AND DISCUSSION

All samples were single phase with the hexagonal $P6_3cm$ structure at room temperature. Figure 1 shows the Rietveld refinement for the $YMnO_3$ XRD pattern with $R_p=9$, $R_{wp}=12$, and $\chi^2=1.6$ using the FULLPROF program. Both for $HoMn_{1-x}Ga_xO_3$ and $YMn_{1-x}Ga_xO_3$, the lattice parameter a decreases and c increases with increasing x as shown in the inset of Fig. 1.

Figure 2 shows the temperature dependence of C_p for $HoMn_{1-x}Ga_xO_3$. The data show three anomalies: (i) a λ-type anomaly at T_N; (ii) a narrow peak around T_{SR}, Fig. 3(a); and (iii) a sharp peak at T_2, Fig. 3(b). With increasing x, T_N and T_2 decrease but T_{SR} increases. All of the transition temperatures obtained from $C_p(T)$ are in agreement with the temperatures obtained by former dc susceptibility and dielectric constant measurements reported before.[15] $C_p(T)$ of $YMn_{1-x}Ga_xO_3$ just shows a λ-type peak at T_N, Fig. 4, which decreases with increasing x. For the $YMn_{0.7}Ga_{0.3}O_3$ sample, C_p shows no peak with temperature down to 2 K. Another noteworthy feature is that there are broad peaks between 5 K and 10 K for $HoMn_{1-x}Ga_xO_3$, but no such peaks for $YMn_{1-x}Ga_xO_3$. The specific heat for $HoMnO_3$ and $YMnO_3$ presented here are similar to the data obtained from polycrystalline samples or single crystals grown by the flux method.[4,14,16]

The λ-type anomaly at T_N of $YMn_{1-x}Ga_xO_3$ shows the second-order nature of the antiferromagnetic (AFM) transition of the Mn^{3+} magnetic moments. In order to estimate the magnetic entropy near T_N, the phonon contribution has to be

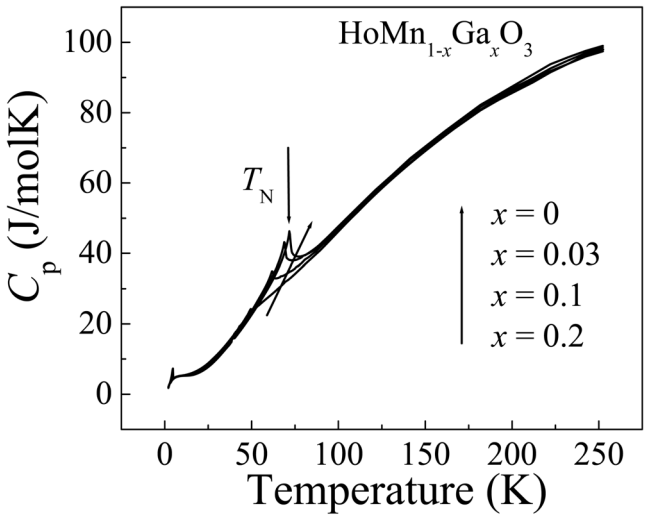

FIG. 2. Temperature dependences of specific heat C_p for $HoMn_{1-x}Ga_xO_3$.

estimated and subtracted from the total specific heat. First we used the Debye formula to calculate the lattice specific heat,

$$C_{lat} = 9RN\left(\frac{T}{\theta_D}\right)^3 \int_0^{\theta_D/T} \frac{x^4 e^x}{(e^x-1)^2} dx, \quad (1)$$

where $N=5$ is the number of atoms in the unit cell, $R=8.314$ J/mol K is the ideal gas constant, and θ_D is the Debye temperature. We chose $\theta_D=628$ K for $YMnO_3$ so that the experimental value of C_p at 250 K coincides with C_{lat}. The calculated C_{lat} is shown by solid line in Fig. 5. The resultant magnetic specific heat associated with ordering of Mn spins at T_N, $C_{Mn}=C_p-C_{lat}$, is plotted as C_{Mn}/T in Fig. 5. For $YMnO_3$, the calculated magnetic entropy from the numerical integration of C_{Mn}/T is $S=19.1$ J/mol K, which is even larger than the maximum value of $R\ln 5=13.4$ J/mol K. Obviously, the Debye formula is not a good estimation for C_{lat} of $YMnO_3$. There are several possible reasons for this discrepancy. The Debye approximation works well for systems dominated by acoustic phonons in the excitation spectrum. It is known from neutron scattering experiments that additional contributions are present from optical modes and magnons, which would alter the Debye spectrum and increase the specific heat. Therefore, other methods of obtaining a more appropriate lattice contribution are needed.

We measured the specific heat of $YMn_{0.7}Ga_{0.3}MnO_3$, which is the single crystal with highest Ga doping we could prepare. C_p of this sample shows no magnetic ordering peak as low as 2 K. At high temperature and low temperature, the specific heat coincides with other $YMn_{1-x}Ga_xO_3$ data, Fig. 4. The mass change of $YMn_{1-x}Ga_xO_3$ due to Ga doping is just around 2%, which doesn't significantly affect the lattice contribution of the specific heat. Therefore, C_p of $YMn_{0.7}Ga_{0.3}MnO_3$ is chosen as the lattice specific heat for $YMn_{1-x}Ga_xO_3$. The resultant magnetic specific heat calculated by this method, $C_{Mn}=C_p-C_{lat}$, is plotted as C_{Mn}/T in Fig. 6. The calculated magnetic entropy for $YMnO_3$ is S

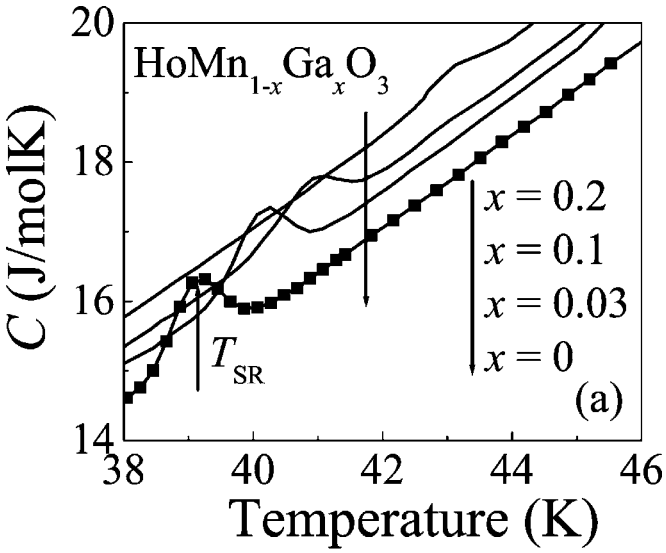

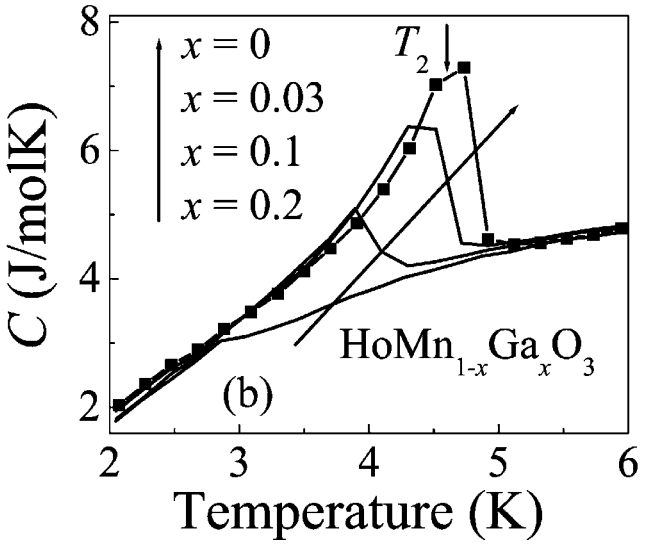

FIG. 3. Temperature dependences of specific heat C_p for $HoMn_{1-x}Ga_xO_3$ around T_{SR} (a) and T_2 (b).

=3.8 J/mol K, which is 28% of $R \ln 5$. We also calculated the fraction of entropy loss above T_N (defined as the maximum in the specific heat curves) in the total magnetic entropy denoted as $S(T_N)/S$. It was found that about 50% of entropy was lost above T_N for $YMnO_3$. The smaller than expected entropy release around T_N and large release of entropy above T_N in $YMnO_3$ is typical of highly degenerate ground states in geometrically frustrated spin systems, which leads to the enhanced spin fluctuations above T_N.[14,17]

For $YMn_{1-x}Ga_xO_3$, the entropy decreases and $S(>T_N)/S$ increases with increasing x, Fig 7. For the $x=0.2$ sample, the transition is obviously broadened and $S(>T_N)/S$ value jumps to 72%. Ga doping in $YMnO_3$ affects the magnetic entropy at T_N in two ways: (i) it reduces the total number of magnetic Mn^{3+} ions to linearly decrease the magnetic entropy; (ii) it reduces the spin fluctuations and leads to a development of short-range magnetic orderings above T_N. The combination of these effects broadens the transition and transfers the entropy release from below to above T_N, which results in the

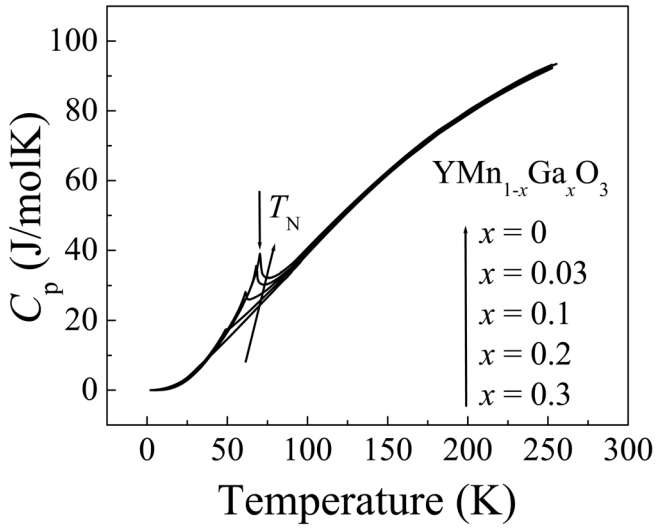

FIG. 4. Temperature dependences of specific heat C_p for $YMn_{1-x}Ga_xO_3$.

increase of $S(>T_N)/S$ with increasing x. The reduction of the spin fluctuations is obtained by the random distribution of Ga ions on the Mn-sites, which dilutes the Mn-Mn interactions and also leads to a decrease of T_N.

Figure 8 shows the magnetic specific heat associated with the transition at T_{SR}, which is plotted as C_{SR}/T. Here C_{SR}/T is obtained by subtracting a linear background fit from C_p/T in a small temperature range near T_{SR}. The observed peaks for the specific heat at T_{SR} are due to the partial AFM orderings of Ho^{3+}-ion spins, which have also been inferred from dc susceptibility and neutron scattering data.[4–6] The reorientation of Mn spins can't account for the entropy change in this temperature region. The calculated $S=0.04$ J/mol K for $HoMnO_3$ is consistent with the value obtained from single crystals grown by the flux method.[4] With Ga doping, T_{SR} increases but the entropy decreases. The increase of T_{SR} actually follows the enhancement of ferrielectricity with Ga

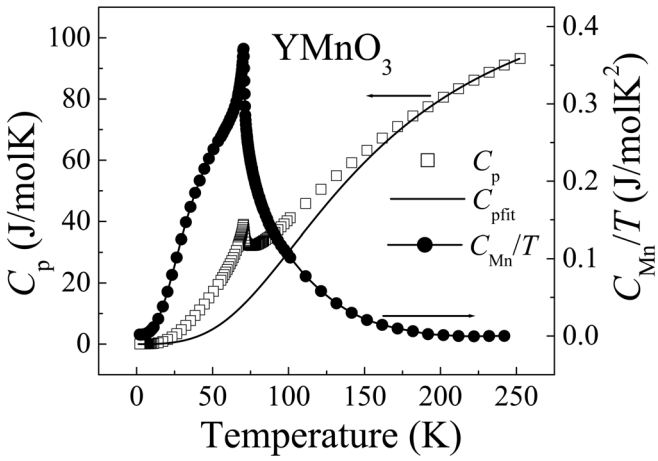

FIG. 5. The fitting result (solid line) and experimental data (open squares) for $YMnO_3$ using the Debye specific heat [Eq. (1)]. C_{Mn}/T is plotted as solid circle.

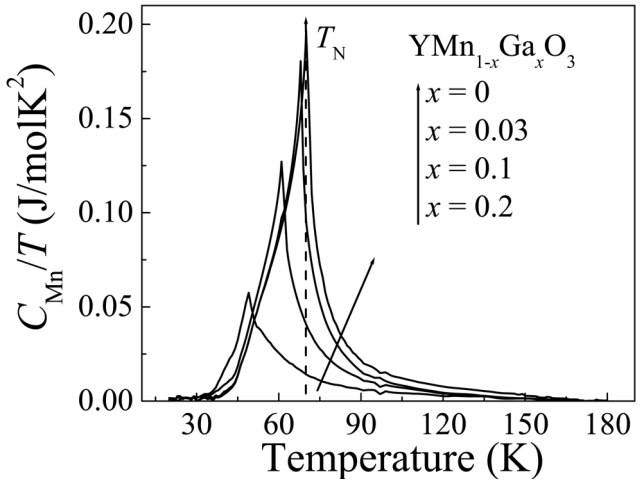

FIG. 6. Temperature dependences of C_{Mn}/T for $YMn_{1-x}Ga_xO_3$. C_{Mn} is obtained by subtracting C_p of $YMn_{0.7}Ga_{0.3}O_3$ from $YMn_{1-x}Ga_xO_3$.

doping.[15] On the other hand, the decrease of the entropy for Ho^{3+}-ion spin ordering with the reduction of Mn-Mn interactions by Ga doping clearly shows the coupling between them. So the multiferrocity at T_{SR} for $HoMn_{1-x}Ga_xO_3$ is not related to the Ho spin ordering: the former occurs at a critical Ho^{3+} displacement, and the latter is driven by the Mn spin ordering.

The broad peak of C_p at low temperature, which only exists in $HoMn_{1-x}Ga_xO_3$, suggests that it is related to the Ho^{3+} ion. Similar behavior has been reported for $PrMnO_3$ and explained as the Schottky effect.[18] Thus, for $T \ll \theta_D$, we may describe C_p as

$$C_p = C_e + C_{ph} + C_{sch}, \tag{2}$$

with

$$C_e = \gamma T, \tag{3}$$

$$C_{ph} = \beta T^3, \tag{4}$$

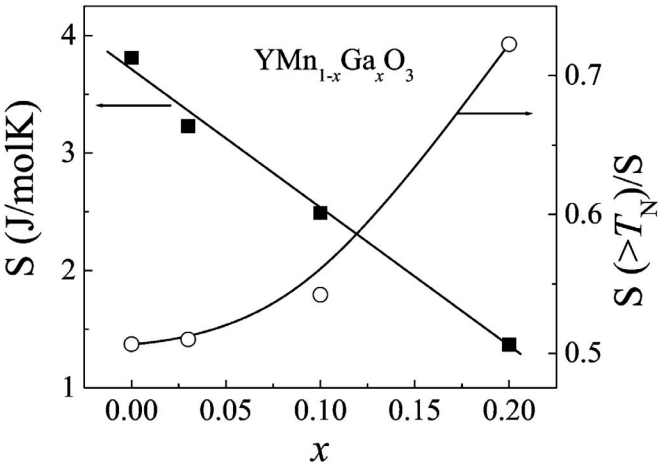

FIG. 7. Variation with x of the calculated entropy (■) and $S(>T_N)/S$ (○) for $YMn_{1-x}Ga_xO_3$.

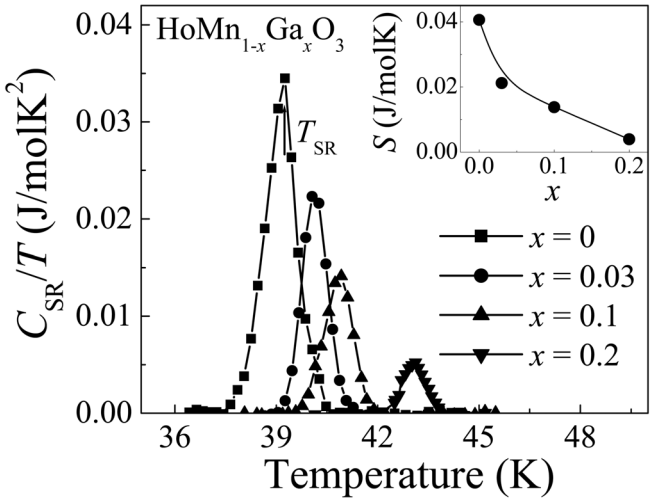

FIG. 8. Temperature dependences of C_{SR}/T for $HoMn_{1-x}Ga_xO_3$. C_{SR} is the magnetic specific heat from the Ho^{3+}-ion spins near T_{SR}. The inset shows the variation with x of the calculated entropy.

$$C_{sch} = \frac{R}{T^2}\left\{\sum_{i=1}^{n}\Delta_i^2 \exp\left(\frac{-\Delta_i}{T}\right) \Big/ \sum_{i=1}^{n}\exp\left(\frac{-\Delta_i}{T}\right) - \left[\sum_{i=1}^{n}\Delta_i \exp\left(\frac{-\Delta_i}{T}\right) \Big/ \sum_{i=1}^{n}\exp\left(\frac{-\Delta_i}{T}\right)\right]^2\right\}. \tag{5}$$

These terms correspond to contributions from electrons, phonons, and Schottky anomalies, respectively. Here, $\beta = N(12/5)\pi^4 R\theta_D^{-3}$ with the same values of R and N as in Eq. (1); Δ_i is the ith energy level of crystal field in Kelvin.[19,20] Recent neutron scattering data[3] indicates two crystal field levels of Ho at 1.5 meV (17.4 K) and 3.1 meV (36 K), so here we chose $i=2$. The solid curves shown in Fig. 9 are fits of experimental data (open circles) and the fitting parameters are listed in Table I. The fitting curves deviate from the experimental data at low temperature near the Ho^{3+} magnetic ordering temperature T_2, which may due to the critical behavior of specific heat near magnetic transition. Several features are noteworthy from the fittings: (i) Δ_1 and Δ_2 derived from the fit are 17.8(2) K and 35.6(2) K for $HoMnO_3$, which are consistent with the 17.4 K and 36 K obtained from the neutron scattering experiment; (ii) $HoMn_{1-x}Ga_xO_3$ samples are insulators at low temperature. Therefore, the magnitude of γ ($0.19 \sim 0.21$ J/mol K^2), which is about two orders larger than the values observed from the free electron contribution, is unusual. Actually the low temperature specific heat of $YMnO_3$ can be fit as $C_p = 1.8 \times 10^{-4}$ J/mol K$^4 \times T^3$, Fig. 9(a), which means γ is nearly zero. A linear term can be expected due to the degenerate ground states in the disordered systems.[21,22] This large γ may be related to the disorder of Ho^{3+} spins above the ordering temperature T_2, which has been shown as a slow increase of the Ho magnetic Bragg peaks between 32 K and 5 K from the neutron scattering data.[6] (iii) β ($1.3 \sim 1.5 \times 10^{-4}$ J mol K^4) doesn't change much with x, which means the small mass change by Ga doping doesn't significantly affect the specific heat. Muñoz *et al.*[5] have reported the specific heat of $HoMnO_3$ and ob-

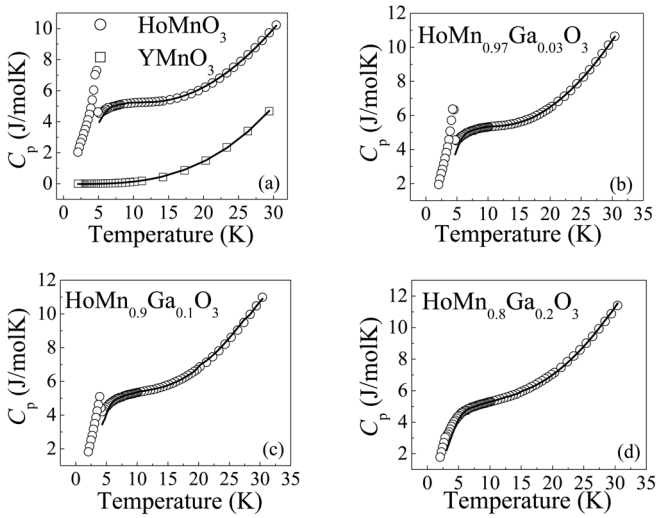

FIG. 9. Temperature dependences of specific heat (open circles) with $2<T<30$ K for $HoMn_{1-x}Ga_xO_3$. The solid lines are fittings using Eq. (2). The open squares in (a) are the experimental data of $YMnO_3$ and the solid line is the fit as $C_p=1.8\times10^{-4}$ J/mol K^4 $\times T^3$.

tained $\gamma=0.386$ J/mol K^2 and $\beta=5\times10^{-5}$ J/mol K^4, but they had no comments on this large γ. The reason for the inconsistency of the values of γ and β between their results and ours may be that in Ref. 5 the data was taken on polycrystalline sample and fit between 30 and 60 K, but we took the data on single crystal and fit the data below 30 K. (iv) the similar magnitude of Δ value for different x also suggests that C_{sch} is dominated by crystal field effects from the Ho^{3+} ion. The decrease of the Δ value with increasing x reflects that the splitting of the energy levels decreases slightly with the dilution of the Mn-Mn interactions. This result shows that an internal field created by Mn spin ordering also affects the Schottky anomaly.

TABLE I. Parameters obtained from the fit of experimental data to Eq. (2) for $HoMn_{1-x}Ga_xO_3$.

x	γ (J/mol K^2)	β_3 (10^{-4} J/mol K^4)	Δ_1 (K)	Δ_2 (K)
0	0.19(3)	1.3(1)	17.8(2)	35.6(2)
0.03	0.20(1)	1.3(1)	16.2(1)	33.6(2)
0.1	0.21(2)	1.4(2)	15.0(2)	32.1(1)
0.2	0.21(1)	1.5(1)	13.0(1)	31.0(2)

Below 5 K, the sharp increase of specific heat around T_2 is due to the long-range magnetic ordering of the Ho^{3+} spins. A decrease with x of T_2 like that of T_N and the magnitude of the peak in $C_p(T)$ at T_2 suggest that the Ho^{3+}-ion spins are coupled to the Mn^{3+}-ion order.

CONCLUSIONS

In conclusion, based on the present specific heat studies of $RMn_{1-x}Ga_xO_3$ (R=Ho, Y), it has been demonstrated that (i) strong spin fluctuations exist above T_N in the GF spin system and Ga doping enhances the short-range ordering; (ii) a coupling between Mn and Ho spin orderings exists at T_{SR} and T_2, but an uncoupling occurs between ferrielectricity and Ho spin ordering at T_{SR}; (iii) a Schottky anomaly of $HoMn_{1-x}Ga_xO_3$ that is dominated by the crystalline electric fields but is also affected by Mn spin orderings; (iv) the large γ contribution in $HoMnO_3$ is most likely due to spin disorder on the Ho site.

ACKNOWLEDGMENTS

This work is supported by a contractual agreement between the NSF and the State of Florida through NHMFL. L. Balicas acknowledges support from the NHMFL in-house research program. We thank Eric Lochner at MARTECH of FSU for assistance with XRD measurements.

[1] P. Coeuré, P. Guinet, J. C. Peuzin, G. Buisson, and E. F. Bertaut, *Proceedings of the International Meeting on Ferroelectricity*, edited by V. Dvorák, A. Fousková, and P. Glogar (Institute of Physics of the Czechoslovak Academy of Science, Prague 1966), Vol. 1, pp. 332–340.
[2] M. Fiebig, Th. Lottermoser, and R. V. Pisarev, J. Appl. Phys. **93**, 8194 (2003).
[3] O. P. Vajk, M. Kenzelmann, J. W. Lynn, S. B. Kim, and S.-W. Cheong, Phys. Rev. Lett. **94**, 087601 (2005).
[4] B. Lorenz, F. Yen, M. M. Gospodinov, and C. W. Chu, Phys. Rev. B **71**, 014438 (2005).
[5] A. Muñoz, J. A. Alonso, M. J. Martínez-Lope, M. T. Casáis, J. L. Martínez, and M. T. Fernández-Díaz, Chem. Mater. **13**, 1497 (2001).
[6] Th. Lonkai, D. Hohlwein, J. Ihringer, and W. Prandl, Appl. Phys. A: Mater. Sci. Process. **A74**, 843 (2002).
[7] Th. Lottermoser, Th. Lonkai, U. Amann, D. Hohlwein, J. Ihringer, and M. Fiebig, Nature (London) **430**, 541 (2004).
[8] M. Fiebig, D. Fröhlich, K. Kohn, St. Leute, Th. Lottermoser, V. V. Pavlov, and R. V. Pisarev, Phys. Rev. Lett. **84**, 5620 (2000).
[9] M. Fiebig, C. Degenhardt, and R. V. Pisarev, J. Appl. Phys. **91**, 8867 (2002).
[10] F. Yen, C. R. dela Cruz, B. Lorenz, Y. Y. Sun, Y. Q. Wang, M. M. Gospodinov, and C. W. Chu, Phys. Rev. B **71**, 180407(R) (2005).
[11] Seongsu Lee, A. Pirogov, Jung Hoon Han, J.-G. Park, A. Hoshikawa, and T. Kamiyama, Phys. Rev. B **71**, 180413(R) (2005).
[12] C. R. dela Cruz, F. Yen, B. Lorenz, Y. Q. Wang, Y. Y. Sun, M. M. Gospodinov, and C. W. Chu, Phys. Rev. B **71**, 060407(R) (2005).
[13] B. Lorenz, A. P. Litvinchuk, M. M. Gospodinov, and C. W. Chu, Phys. Rev. Lett. **92**, 087204 (2004).
[14] T. Katsufuji, S. Mori, M. Masaki, Y. Moritomo, N. Yamamoto,

and H. Takagi, Phys. Rev. B **64**, 104419 (2001).
[15] H. D. Zhou, J. C. Denyszyn, and J. B. Goodenough, Phys. Rev. B **72**, 224401 (2005).
[16] M. Tachibana, J. Yamazaki, H. Kawaji, and T. Atake, Phys. Rev. B **72**, 064434 (2005).
[17] J. E. Greeden, J. Mater. Chem. **11**, 37 (2001).
[18] J. G. Cheng, Y. Sui, X. J. Wang, Z. G. Liu, J. P. Miao, X. Q. Huang, Z. Liu, Z. N. Qian, and W. H. Su, J. Phys.: Condens. Matter **17**, 5869 (2005).
[19] Y. M. Jana, O. Sakai, R. Higashinaka, H. Fukazawa, Y. Maeno, P. Dasgupta, and D. Ghosh, Phys. Rev. B **68**, 174413 (2003).
[20] V. Sima, M. Davis, P. Svoboda, Z. Smetana, S. Zajac, and J. Bischofl, J. Phys.: Condens. Matter **1**, 10153 (1989).
[21] P. Raychaudhuri, C. Mitra, A. Paramekanti, R. Pinto, A. K. Nigam, and S. K. Dhar, J. Phys.: Condens. Matter **10**, L191 (1998).
[22] L. Ghivelder, I. A. Castillo, M. A. Gusmão, J. A. Alonso, and L. F. Cohen, Phys. Rev. B **60**, 12184 (1999).